

The Small Subunit of the Mammalian Mitochondrial Ribosome

IDENTIFICATION OF THE FULL COMPLEMENT OF RIBOSOMAL PROTEINS PRESENT*

Received for publication, January 25, 2001, and in revised form, February 26, 2001
Published, JBC Papers in Press, March 2, 2001, DOI 10.1074/jbc.M100727200

Emine Cavdar Koc‡, William Burkhardt§, Kevin Blackburn§, Arthur Moseley§, and
Linda L. Spremulli‡¶

From the ‡Department of Chemistry and Campus Box 3290, University of North Carolina, Chapel Hill, North Carolina 27599-3290 and §GlaxoSmithKline Research and Development, Department of Structural Chemistry, Research Triangle, North Carolina 27709-3398

Identification of all the protein components of the small subunit (28 S) of the mammalian mitochondrial ribosome has been achieved by carrying out proteolytic digestions of whole 28 S subunits followed by analysis of the resultant peptides by liquid chromatography and tandem mass spectrometry (LC/MS/MS). Peptide sequence information was used to search the human EST data bases and complete coding sequences of the proteins were assembled. The human mitochondrial ribosome has 29 distinct proteins in the small subunit. Fourteen of this group of proteins are homologs of the *Escherichia coli* 30 S ribosomal proteins S2, S5, S6, S7, S9, S10, S11, S12, S14, S15, S16, S17, S18, and S21. All of these proteins have homologs in *Drosophila melanogaster*, *Caenorhabditis elegans*, and *Saccharomyces cerevisiae* mitochondrial ribosomes. Surprisingly, three variants of ribosomal protein S18 are found in the mammalian and *D. melanogaster* mitochondrial ribosomes while *C. elegans* has two S18 homologs. The S18 homologs tend to be more closely related to chloroplast S18s than to prokaryotic S18s. No mitochondrial homologs to prokaryotic ribosomal proteins S1, S3, S4, S8, S13, S19, and S20 could be found in the peptides obtained from the whole 28 S subunit digests or by analysis of the available data bases. The remaining 15 proteins present in mammalian mitochondrial 28 S subunits (MRP-S22 through MRP-S36) are specific to mitochondrial ribosomes. Proteins in this group have no apparent homologs in bacterial, chloroplast, archaeobacterial, or cytosolic ribosomes. All but two of these proteins have a clear homolog in *D. melanogaster* while all but three can be found in the genome of *C. elegans*. Five of the mitochondrial specific ribosomal proteins have homologs in *S. cerevisiae*.

Mammalian mitochondria carry out the synthesis of 13 polypeptides that are essential for oxidative phosphorylation and, hence, for the synthesis of the majority of the ATP used by eukaryotic organisms. The ribosomes present in mammalian mitochondria are 55–60 S particles and are composed of small (28 S) and large (39 S) subunits (1). They are characterized by a low percentage of rRNA and a compensating increase in the number of ribosomal proteins (2, 3). The small subunit of the

ribosome contains a 12 S rRNA and about 30 proteins while the large subunit consists of a 16 S rRNA and about 50 proteins (4, 5). The number of proteins present is significantly higher than that observed in bacterial ribosomes.

Recently, 18 proteins from the large subunit and 17 proteins from the small subunit of the mammalian mitochondrial ribosome have been characterized. The analysis of these proteins was carried out primarily following separation of the proteins on two-dimensional gels. Sequence information on the separated proteins was obtained by Edman degradation or by sequencing proteolytic products using Edman chemistry or mass spectrometry. The data obtained was used extensively to probe the EST data bases and the full-length cDNAs and the corresponding amino acid sequences were then assembled (6–13). Of these proteins, 12 from the large subunit and 6 from the small subunit are homologs of bacterial ribosomal proteins. The remainder fall into new classes of ribosomal proteins.

The identification of proteins in mammalian mitochondrial ribosomes has been challenging due to their low abundance. The traditional approach to sequence the proteins present has been to separate them using two-dimensional gels or high performance liquid chromatography. Individual proteins are then digested and sequence obtained on the peptides generated. In the present study, we have combined this approach with a streamlined analysis involving proteolytic digestions of whole 28 S subunits. Sequence information on peptides present in this complex mixture was obtained by liquid chromatography coupled to tandem mass spectrometry. The sequence information obtained was used in data base searches to allow the deduction of the complete amino acid sequences of these proteins. A related approach has recently been reported for the analysis of the protein composition of yeast cytoplasmic ribosomes (14). The approach used here allowed us to identify 14 new mammalian mitochondrial ribosomal proteins. Of these, 10 have homologs in prokaryotic ribosomes (including three variants of ribosomal protein S18) while 4 are members of new classes of small subunit ribosomal proteins. This work and previous efforts have led to what we believe is the complete identification of all the proteins in the small subunit of the mammalian mitochondrial ribosome.

MATERIALS AND METHODS

Preparation of Bovine Mitochondrial Ribosomal Proteins for Two-dimensional Gel Electrophoresis—Bovine mitochondria and 28 S subunits were prepared as described previously by Matthews *et al.* (4) and the 28 S subunits were collected by centrifugation at 48,000 rpm for 6 h in a Beckman Type-50 rotor. For analysis of individual proteins separated on two-dimensional gels, samples were prepared as described previously prior to loading on nonequilibrium pH gradient tube gels (5, 8). For analysis of proteins in whole 28 S subunit preparations, 55 S mitochondrial ribosomes were isolated on sucrose gradients (4). These

* This work has been supported by National Institutes of Health Grant GM32734. The costs of publication of this article were defrayed in part by the payment of page charges. This article must therefore be hereby marked "advertisement" in accordance with 18 U.S.C. Section 1734 solely to indicate this fact.

¶ To whom correspondence should be addressed. Tel.: 919-966-1567; Fax: 919-966-3675; E-mail: Linda_Spremulli@unc.edu.

ribosomes were diluted in buffer containing 20 mM Tris-HCl, pH 7.6, 2 mM MgCl₂, 40 mM KCl, and 2 mM dithiothreitol to dissociate the 55 S ribosomes into 28 S and 39 S subunits. Two-ml samples were then applied to 36-ml linear gradients (10 to 30% sucrose in the above buffer). Samples were subjected to centrifugation for 16 h at 24,000 rpm in a SW27 rotor. The gradients were fractionated and 28 S subunits were collected by centrifugation at 48,000 rpm for 6 h. The 28 S subunit pellet was resuspended in 0.1 ml of buffer containing 20 mM Tris-HCl, pH 7.6, 5 mM MgCl₂, 40 mM KCl, and 2 mM dithiothreitol and stored at -70 °C.

Peptide Sequencing by Mass Spectrometry—Randomly picked spots from the two-dimensional polyacrylamide gel electrophoresis of the mitochondrial ribosomal small (28 S) subunit were excised and digested in-gel with trypsin (Roche Molecular Biochemicals, Basel, Switzerland) as described previously (9, 12, 15). Nanoscale capillary liquid chromatography-tandem mass spectrometric (LC/MS/MS)¹ analyses of in-gel digests were done using an Ultimate capillary LC system (LC Packings, San Francisco, CA) coupled to a quadrupole time-of-flight (Q-TOF) mass spectrometer (Micromass, Manchester, United Kingdom) fitted with a Z-spray ion source as described previously (8).

For analysis of proteins in whole small subunits, 3 pmol of 28 S subunits (isolated by sucrose density gradient centrifugation following the dissociation of 55 S particles) were subjected to endoprotease Lys-C (Wako BioProducts, Richmond VA) digestion (16). The peptides that were obtained from the whole 28 S subunit digests were analyzed by nanoscale capillary LC/MS/MS with and without a variable-flow LC/MS interface.² Uninterpreted peptide product ion spectra generated by LC/MS/MS were searched against the nonredundant protein data base and EST data bases for exact matches using the Mascot search program (17). High quality spectra which had no exact matches in either the protein or EST data bases were sequenced *de novo* either manually or with the aid of the PepSeq program (Micromass). In manual sequencing, ions originating from the C terminus (y' ion series) or from the N terminus (b ion series) formed by cleavage of the amide bonds along the peptide backbone were identified. Adjacent y' or b ions differ by the corresponding amino acid residue mass, enabling assignment of peptide amino acid sequence.

Computational Analysis—Peptide sequences obtained from Mascot searches of the protein and EST data bases and those obtained by *de novo* sequencing were searched against the nonredundant protein data base using the FASTA algorithm (18). For peptides with no exact matches in the data bases, sequences obtained by *de novo* sequencing were used for FASTA searches. Because mass spectrometry cannot distinguish between amino acids Leu and Ile which have the same residue masses, initial data base searches were carried out using Leu in the peptide sequences. Hits with an Ile at these positions were considered exact matches. If no hits were obtained with Leu in the query sequence, the search was redone with Ile. The isobaric (same nominal molecular weight) amino acids Phe and oxidized Met (a common artifact of polyacrylamide gel electrophoresis) were distinguished by diagnostic loss of methanesulfonic acid (64 Da) from oxidized Met (19). Because the protease endoprotease Lys-C which cleaves on the C-terminal side of Lys residues was used for in-gel and *in situ* digestions, Lys residues could be distinguished with a fairly high certainty from isobaric Gln residues.

EST data base and genomic DNA searches of the peptide sequences were performed using the BLAST search program (20). Sequence analysis and homology comparisons were done using the GCG DNA analysis software package (44), Vector NTI (Informax Inc.), and Biology Work-Bench 3.2. The results were displayed using BOXSHADE (version 3.21, written by K. Hofmann and M. Baron). Prediction of the cleavage sites for the mitochondrial signal sequence was carried out using PSort and MitroProt II (21, 22).

RESULTS

Nomenclature

Two-dimensional gel analysis of the proteins present in bovine liver mitochondrial 28 S subunits suggested the presence of as many as 33 ribosomal proteins. These proteins were designated S1 to S33 in order of decreasing molecular weight (4). However, as protein sequence information became avail-

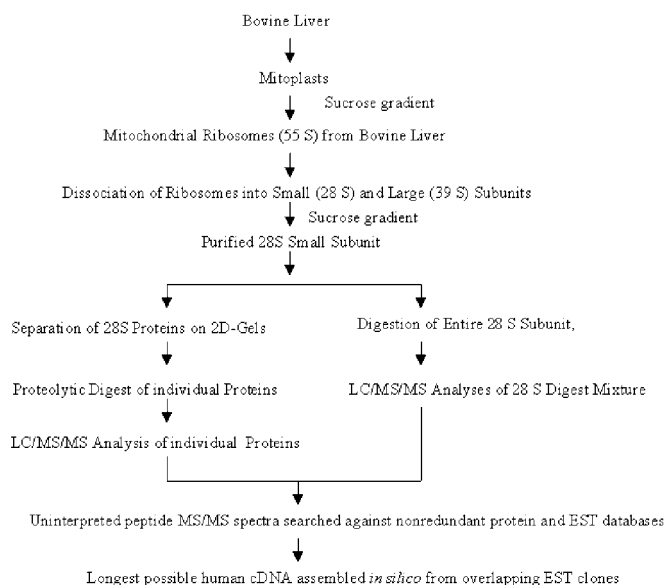


FIG. 1. Strategies used for the identification of the mitochondrial ribosomal proteins. Bovine mitochondrial 28 S ribosomal subunits were purified using two sequential sucrose gradients. Several of the ribosomal proteins were identified following separation of individual proteins on two-dimensional gels. Most of the ribosomal proteins were identified in proteolytic digests of whole 28 S subunits followed by direct analysis using LC/MS/MS.

able, it became clear that designating mammalian mitochondrial ribosomal proteins in this way does not provide a consistent nomenclature for these proteins from different mammals. For example, bovine MRP-S18 is the same protein as rat MRP-S13 (11). To simplify the literature and to facilitate the comparisons of mitochondrial ribosomal proteins to those from other translational systems, we are using a system of nomenclature similar to that recently adopted for chloroplast ribosomal proteins (23, 24). In this system, proteins with prokaryotic homologs are given the same number as the corresponding ribosomal protein in *E. coli*. For example, MRP-S7 is the mammalian mitochondrial homolog of bacterial S7. Proteins without bacterial homologs are given the next available number. Since there are 21 proteins in the bacterial ribosome, we began designating the new mammalian mitochondrial ribosomal proteins beginning at MRP-S22 (9, 12, 13). In previous work, we identified 9 bovine mitochondrial small subunit mitochondrial ribosomal proteins that do not have prokaryotic homologs and used the designations MRP-S22 through MRP-S30. The current manuscript describes 10 homologs of bacterial ribosomal proteins and four new class small subunit ribosomal proteins, MRP-S31, MRP-S32, MRP-S33, and MRP-S36.

Characterization of Bovine Mitochondrial Ribosomal Proteins by Tandem Mass Spectrometry

The strategies used here to identify and characterize bovine mitochondrial ribosomal proteins are summarized in Fig. 1. The traditional approach used to identify proteins present in complex mixtures has been to separate them on two-dimensional gels. Individual protein spots are then subjected to proteolytic digestion and peptide sequence information obtained on them. This strategy was used in previous studies to obtain the sequences of 10 small subunit ribosomal proteins (8, 9, 12). In the current work, an additional ribosomal protein has been identified using this method.

To streamline the analysis of additional proteins present in 28 S subunits, whole subunits were subjected to proteolytic digestion. The resulting peptide mixture was analyzed by nanoscale capillary LC/MS/MS using a quadrupole time-of-

¹ The abbreviation used is: LC/MS/MS, liquid chromatography-tandem mass spectrometry.

² J. P. C. Vissers, M. A. Moseley, and R. K. Blackburn, manuscript in preparation.

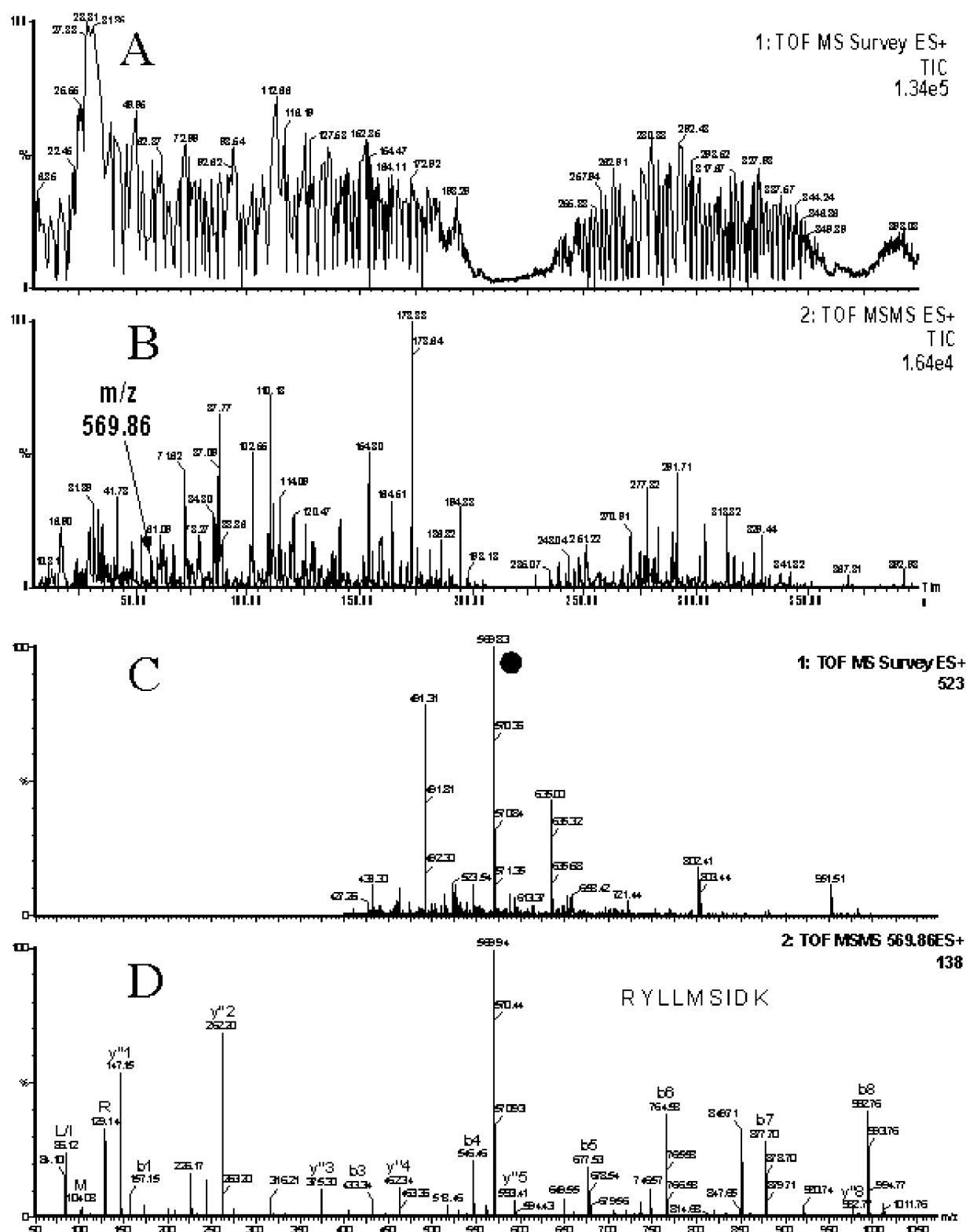


FIG. 2. Variable flow nanoscale capillary LC/MS/MS analysis of an *in situ* Lys-C digestion of the 28 S subunit. *A*, total ion chromatogram obtained from the whole digest of 28 S subunits illustrating detection of material eluting from the LC column. The “spikes” in the data in the MS survey here are due to the almost constant switching of the instrument between MS and MS/MS modes during data acquisition of this extremely complex mixture of peptides. The *x* axis is the time in min of the elution from the LC column. *B*, total ion chromatograms obtained for the MS/MS scan function indicating the elution times (in min) of peptides of potential interest. *C*, the MS spectrum obtained in the MS survey scan taken at 57 min. The most abundant ion in this spectrum (*m/z* 569.8) was subjected to MS/MS analysis as shown in *D*. A Mascot search of the protein/EST data bases found that a peptide (RYLLMSIDK) from MRP-S15 matched this product ion spectrum.

flight mass spectrometer with data-dependent MS to MS/MS switching (Fig. 1). With this method, peptides derived from 28 S subunits are eluted from a reversed-phase nanoscale capil-

lary LC column into the source of the mass spectrometer. The MS is used much like a UV monitor to detect material eluting from the column (Fig. 2A) and to determine the location of

TABLE I

Amino acid sequences of mature MRPs of *Bos taurus* deduced from database searching of peptide product ion spectra from whole 28 S subunits

Sequence	<i>m/z</i>	Protein match	Swiss-Protein number	
			Bovine	Human
FMEPYIFGSR	1245.69	MRP-S2	P82923	Q9Y399
ECEGIVPVPLEEK	1545.77	MRP-S6	P82931	P82932
AMQRPETAAALK	1285.68	MRP-S6		
GTGIAAQTAGIAAAAK	1370.86	MRP-S11	P82911	P82912
KFEEIPIAHIK	1323.60	MRP-S11		
ASCGTEGFR	1031.31	MRP-S11		
DYQNVPGIEK	1161.42	MRP-S15	P82913	P82914
DYQNVPGIEKVDDVVK	1816.74	MRP-S15		
RLLSLEMANK	1173.76	MRP-S15		
RYLLMSIDK	1137.62	MRP-S15		
ALCIRVFQEVQK	1537.84	MRP-S15		
ELGIEYTFPPPYHRK	1845.94	MRP-S15		
EQAAEGLQLIK	1198.66	MRP-S15		
TNYPVFEK	996.56	MRP-S15		
..LEAQLVAL.. ^a	1573.68	MRP-S15		
YLLMSIDQR	1137.72	MRP-S15		
..PMPNSHADK.. ^a	2822.92	MRP-S16	P82915	Q9Y3D3
RAQEVLLAAQK	1225.71	MRP-S16		
TYFAHDALEQCTVGDIVLLK	2339.20	MRP-S17	P82916	Q9Y2R5
HELAEIVFK	1084.59	MRP-S17		
HVKHELAEIVFK	1448.81	MRP-S17		
VGQVVDVPTGK	1097.61	MRP-S17		
RCAGTTYLESPVDLETTPLAK	2369.31	MRP-S17		
SITGLCQEEHR	1376.41	MRP-S18(1)	P82917	Q9Y3D5
HITGLCGK	932.40	MRP-S18(1)		
QVTSSESLPIPMENPYK	1947.04	MRP-S18(1)		
QVTSSEDLPIPMENPYKEPLK	2414.33	MRP-S18(1)		
ARDHGLLSYHIPQVEPR	1986.59	MRP-S18(2)	P82918	Q9Y676
APPEDSLPPIPVSPYEDEPWK	2477.16	MRP-S18(2)		
MAVGSPLLKDNVSYTGRPLVLYH	2528.66	MRP-S18(3)	P82919	Q9NVS2
INFLMRK	920.49	MRP-S21	P82920	P82921
YYEKPCR	1062.40	MRP-S21		
NRADPWQGC	1150.37	MRP-S21		
QDWLILHIPDAHLWVK	1983.07	MRP-S29	P82922	P51398
KSPLTPEELLQ	1856.82	MRP-S29		
SPNTPEELALLQ ^b	1856.76	MRP-S29		
PLEAVTWLK	1729.86	MRP-S29		
AYLPQELLGK	1130.63	MRP-S29		
LQTSLNNDARQH	2116.96	MRP-S29		
TVFPHGLPPRFVMQVK	1852.02	MRP-S29		
NTNFAHPAVRYVLYGEK	1978.01	MRP-S29		
HGEQHVGHYNIQELK	2116.04	MRP-S29		
AAPVARYPPIVASLTADSK	1926.06	MRP-S30	P82924	Q9NP92
YPPIVASLTADSK	1360.72	MRP-S30		
NICWGTQSMPLYETIEDNDVK	2560.16	MRP-S30		
ISFSNIISDMK	1253.46	MRP-S31	P82925	Q92665
QGPIRHFMELVTCGLSK	2019.66	MRP-S31		
VEHIEWFRNYFNEK	1910.07	MRP-S31		
LWEFFPINNEAGFDDDDGSEFHEHIFLDK	3219.80	MRP-S31		
YLEGFPK	852.52	MRP-S31		
QLAAVTEQPFQNGFEEMIQWTK	2594.13	MRP-S31		
SKQLEHGPMIEQLSK	1724.67	MRP-S32	P82927	Q9Y6G3
LFSEQPLAK	1031.46	MRP-S33	P82926	Q9Y291
AWGILTFK	934.60	MRP-S34	P82929	P82930
LVIGRIFHIVENDLYID	2416.86	MRP-S35	P82928	Q9Y2Q9
ANLNIEIHK	914.58	MRP-S35		
SPDWLMHQGPPDTAEMIK	2052.02	MRP-S36	P82908	P82909
LVSQEEIEFIQRGGPE	1830.03	MRP-S36		

^a Internal sequences of a peptide fragment.^b *De novo* sequenced peptide product ion spectra.

peptides of potential interest (Fig. 2B). A representative analysis of one of the peptides obtained is shown in Fig. 2C. In this example, the MS spectrum of the peak eluting at ~57 min (labeled in Fig. 2B) is analyzed. This peak has an abundant ion at *m/z* 569.8. The sequence of this peptide was obtained from the product ion fragmentation spectrum obtained from MS/MS analysis (Fig. 2D).

The spectrum illustrated in Fig. 2D, and all other product ion spectra, were initially searched against the nonredundant protein and EST data bases using the Mascot search program (17). This program searches for peptide sequences from entries in the data bases which would generate product ion spectra

matching the fragmentation patterns observed in the individual spectrum. For the spectrum in Fig. 2D, for example, the Mascot program returned the sequence RYLLMSIDK from MRP-S15 as an exact match. For those spectra without exact matches from Mascot, the product ion spectra were manually sequenced *de novo* (see "Materials and Methods").

The approach used here provided a large amount of new peptide sequence information which is summarized in Table I. Peptide sequences obtained from the previously identified mitochondrial ribosomal proteins are not included in this table to simplify the presentation of the data. Sequences of the peptides (Table I) were used to search the human EST data base using

TABLE II
 Characteristics of human mitochondrial ribosomal proteins

Human protein	No. of amino acids	Full-length molecular mass	% Prob. ^a	Predicted PSORT	Cleavage site MitoProtII	Mature protein
		<i>kDa</i>				<i>kDa</i>
MRP-S2	296	33.3	99.3	R-240	48	28.3
MRP-S5	430	48	78	R-286	87	38.9
MRP-S6	125	14.2	19.3	R-24	NP ^b	13.7
MRP-S7	242	28.2	98.7	R-237	37	24.1
MRP-S9	387	44.8	95.1	R-251	51	38.8
MRP-S10	200	22.6	90.4	R-214	NP	21.4
MRP-S11	194	20.6	99.7	R-239	28	17.4
MRP-S12	138	15.2	99.5	R-295	91	12.5 ^c
MRP-S14	128	15.1	77.4	R-227	NP	12.3
MRP-S15	257	31.6	99.8	R-263	57	23.5
MRP-S16	137	15.3	96.9	R-234	34	11.5
MRP-S17	130	14.5	97.8	R-247	20	12.4
MRP-S18(1)	142	15.9	85.8	R-239	39	11.8
MRP-S18(2)	258	29.3	98.5	R-225	25	26.5
MRP-S18(3)	196	22.2	90.6	R-234	37	18.4
MRP-S21	87	10.7	21	R-211	NP	9.4
MRP-S22	360	41.3	71.6	R-1052	29	38.1
MRP-S23	190	21.8	9	R-26	NP	21.1
MRP-S24	166	18.9	91.8	R-235	35	15.1
MRP-S25	151	17.7	80.1	R-212	NP	18.6
MRP-S26	205	24.2	98	R-231	31	20.8
MRP-S27	414	47.7	95.9	R-228	36	43.8
MRP-S28	323	36.8	95.1	R-1021	29	33.8
MRP-S29	397	45.6	91.8	R-229	16	43.6
MRP-S30	439	50.4	84.2	R-29	NP	48.5
MRP-S31	395	45.3	93.4	R-259	67	37.9
MRP-S32	142	6.7	95.2	R-214	NP	15.1
MRP-S33	106	12.6	85.6	R-225	26	9.7
MRP-S34	218	25.7	91	R-1044	18	23.6
MRP-S35	187	20.8	87.8	R-228	28	17.6
MRP-S36	102	11.3	33	R-224	NP	8.7

^a (% Prob), percent probability of import into the mitochondria predicted by MitoProt II and PSORT.

^b NP, not predicted.

^c Despite the predicted cleavage sites, alignment of MRP-S12 with its prokaryotic homolog suggests that the N-terminal homology starts at residue 30, therefore, the molecular weight of the mature MRP-S12 calculated based on the cleavage of the first 30 residues.

the tBLASTN program (National Center for Biotechnology Information). In most cases a number of EST clones gave positive hits for these sequences. Overlapping clones for these hits were obtained using the initial hits as virtual probes to rescreen the human EST data base. Consensus cDNAs were then assembled by repetitive searching and comparison of the EST sequences. Sequencing errors were corrected as much as possible by comparison of overlapping clones. Where possible, EST assemblages from the TIGR data base were examined and used to facilitate the assembly of the full-length sequences and to help evaluate potential sequencing errors in the EST clones. The sequence of the longest possible cDNA was then assembled *in silico*. Generally, the fully assembled human sequence was used as a query against entries in the mouse ESTs and *Caenorhabditis elegans* and *Drosophila melanogaster* genomic data bases.

The peptide sequence information obtained allowed the identification of 8 new homologs of prokaryotic ribosomal proteins, one of which (S18) is present in three variants bringing the total number of new bacterial homologs identified to 10. In addition, 4 novel small subunit ribosomal proteins were identified belonging to new classes. The new sequence information provided here brings the total number of 28 S subunit ribosomal proteins to 31. In addition, with one exception (MRP-S12), all of the previously identified mammalian mitochondrial small subunit ribosomal proteins were identified. The large number of proteins identified using this approach illustrates the power of this method for the analysis of complex protein mixtures.

Since there are three variants of S18, only one of which is presumably present in each small subunit, each subunit would have a complement of 29 ribosomal proteins. Previously 33 potential small subunit ribosomal proteins were reported by Matthews *et al.* (4, 25) based on two-dimensional gel patterns.

This value probably represents an overestimation of the number of proteins in the small subunit. This overestimation could be due to contamination of small subunit preparations with large subunit ribosomal proteins.³ Additional putative small subunit proteins appearing as bands on two-dimensional gels could also arise from modified (and/or partially degraded) small subunit proteins. Only a few peptides from known nonribosomal proteins were observed in our 28 S subunit preparations. These peptides represent about 1% of the total spectrum of peptides observed. These peptides originate from two proteins expected to be associated with ribosomes (the chaperones Hsp60 and Hsp70). In addition, peptides were observed from the subunits of the pyruvate dehydrogenase complex. This large oligomeric complex sediments at 32 S (26) which is around the same buoyant density as ribosomal subunits. We believe that the peptide sequence data obtained here combined with the sequences reported previously allows the identification of essentially all of the proteins in the 28 S subunit of the mammalian mitochondrial ribosome.

The molecular weights of the proteins in the small subunit (following removal of the predicted signal sequence) range from 8.7 to 48.5 kDa (Table II). This range of sizes is in good agreement with the previous spectrum observed in bovine mitochondrial small subunits (4, 25). We have not observed any of the higher molecular mass ribosomal proteins (greater than 49 kDa) reported in rat liver mitochondrial ribosomes by Cahill *et al.* (5). The total calculated molecular mass of the small subunit proteins following removal of the proposed N-terminal signal sequence and using an average molecular mass for the three

³ E. C. Koc, W. Burkhart, K. Blackburn, A. Moseley, and L. L. Spremulli, manuscript in preparation.

S18 variants is about 680 kDa. This value combined with the mass of the 12 S rRNA present in the small subunit (about 315 kDa) brings the total estimated molecular mass of the small subunit to 995 kDa. This value is in good agreement with the protein content of the ribosome calculated from the buoyant density of this subunit and the estimated molecular weights of each individual protein from the two-dimensional gels (4, 25).

TABLE III
Percentage identity of human mitochondrial ribosomal proteins that are also found in other species

Human protein	% Identity to					Ref.
	Mouse	<i>Drosophila</i>	<i>C. elegans</i>	Yeast	<i>E. coli</i>	
MRP-S2	72.8	54.9	34.7	32.8	34.7	This work
MRP-S5	79	46.5	35.3	23.3	24.7	15
MRP-S6	84.8	41.1	24.8	32.5	23.2	This work
MRP-S7	84.6	41	41	19.2	37.3	8
MRP-S9	78.8	33.4	36.5	33	38.6	15
MRP-S10	80.2	44.8	36.4	21.1	30.4	12
MRP-S11	74.4	39.3	36.2	25.7	39.4	This work
MRP-S12	85.5	58.5	46.6	50.4	48.2	42
MRP-S14	86.7	67.6	40.7	30.4	35	12
MRP-S15	62.9	26.8	26.2	26.7	22.7	This work
MRP-S16	91.1	42.2	42.1	38.2	40.2	This work
MRP-S17	84.2	29.8	31.5	24.8	27.7	This work
MRP-S18(1)	82.0	45.3	43.3	26.5	29.6	This work
MRP-S18(2)	78.4	38.7	24.1	22.0	25.7	This work
MRP-S18(3)	80.1	32.1	ND ^a	19.7	26	This work
MRP-S21	90.8	50.0	38.7	21.7	27.5	This work
MRP-S22	78.3	31.4	32.2	ND	ND	12
MRP-S23	76	ND	40.6	ND	ND	12
MRP-S24	81.3	37.4	ND	ND	ND	12
MRP-S25	89.5	56	39.3	24.4	ND	12
MRP-S26	71.4	29.2	ND	ND	ND	6 and 12
MRP-S27	77.1	22.5	22.3	ND	ND	15
MRP-S28	76.8	44.3	37.9	27.1	ND	15
MRP-S29	81.8	37.2	31.9	20.9	ND	13
MRP-S30	74.8	28.1	27.8	ND	ND	13
MRP-S31	66.7	34.7	ND	ND	ND	This work
MRP-S32	75.9	34.5	29.6	ND	ND	This work
MRP-S33	80.2	58.1	43.4	ND	ND	This work
MRP-S34	86.5	24.3	28.7	ND	ND	11
MRP-S35	72.5	40.7	35.1	ND	ND	11
MRP-S36	84.3	ND	25.3	19.4	ND	This work

^a ND, homologs of human ribosomal proteins are not detected in database searches.

The Mitochondrial Small Subunit Proteins with Prokaryotic Homologs

Previous studies had identified 6 homologs of prokaryotic small subunit ribosomal proteins (MRP-S5, MRP-S7, MRP-S9, MRP-S10, MRP-S12, and MRP-S14) in mammalian mitochondrial ribosomes. The present work adds 8 new homologs to this group (MRP-S2, MRP-S6, MRP-S11, MRP-S15, MRP-S16, MRP-S17, MRP-S18(1), MRP-S18(2), MRP-S18(3), and MRP-S21). Thus, a total of 14 small subunit proteins in mammalian mitochondria have bacterial homologs. No proteins corresponding to bacterial ribosomal proteins S1, S3, S4, S8, S13, S19, and S20 could be found either in the catalog of peptide sequences obtained or in extensive searches of the EST data bases using the sequences of these bacterial proteins as probes.

MRP-S2—A single peptide was obtained for MRP-S2 from the proteolytic digestion of whole 28 S subunits (Table I). Initial screening of the EST data bases with this peptide provided a hit with an accession number of AAD34086. However, it was not identified as an S2 homolog. The full-length protein is 296 residues in length and is 34.7% identical to *E. coli* ribosomal protein S2 (Table III). After the removal of the predicted import signal, the sizes of *E. coli* S2 and MRP-S2 are quite comparable (Fig. 3). As might be expected, homologs of MRP-S2 are present in other mammals, *C. elegans*, and *D. melanogaster* (Table III). Of these, the *Drosophila* MRP-S2 is more closely related to the mammalian protein than is *C. elegans* MRP-S2 although this theme is not shared by all of the ribosomal proteins (Table III). Mammalian MRP-S2 is more closely related to its homolog from bacteria than to its *S. cerevisiae* mitochondrial homolog. The low conservation of primary sequence between mammalian and yeast mitochondrial ribosomal proteins has been observed in a number of cases (27).

MRP-S6—Two peptide fragments encoded by the same bovine cDNA (BF041055) were identified as fragments from a protein similar to the prokaryotic S6 ribosomal protein family in Swiss-Prot data base searches (Table I). MitoProt II assigns a low probability for the import of mammalian MRP-S6 into mitochondria (Table II). Interestingly, the yeast mitochondrial homolog, MRP17 (YKL003C), is also assigned a low probability of import into mitochondria and has no signal cleavage motif (27). MRP-S6 is reasonably well conserved (Table III) espe-

FIG. 3. Comparison of molecular weights of *E. coli* 30 S ribosomal proteins with the human mitochondrial small subunit (28 S) ribosomal proteins. The molecular weights of the MRPs are calculated after the removal of putative N-terminal import signals predicted by MitoProt II and/or PSORT. Alignments of MRP-S12 with its prokaryotic homologs suggest that the import signal will not be cleaved (see Table II). Hence, its size is indicated without cleavage. In comparison of molecular weights in the S18 family, MRP-S18(1) has been used.

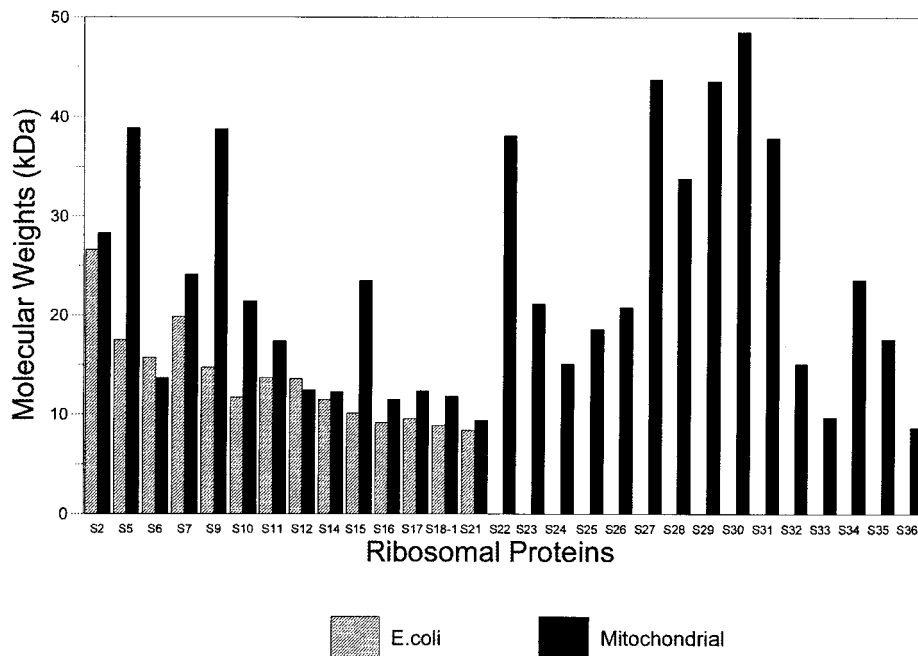


TABLE IV
Accession numbers of mitochondrial ribosomal small subunit proteins found in various species

Accession numbers and/or protein names are reported in GenBank™ and Swiss-Prot databases.

Protein	Human	Drosophila	C. elegans	Yeast	A. thailana
MRP-S2	Q9Y399 (AAD340861)	AAF50970	AAB69935	NP_011859 (YHL004W/Mrp4p)	P56797
MRP-S5	P82675	AA438342 ^a	Q93425	P33759(MRPS5/YBR251W)	?
MRP-S6	P82932	AAF47889	AAC17033	P28778 (YKL003C/MRP17)	AAF19690
MRP-S7	JC7165	AAF52933	T27217	P47150 (YJR113C/Rsm7p)	P56800 (Q9XQ95)
MRP-S9	P82933	AAF54157	P34388	P38120 (MRPS9/YBR146W)	CAB62002 ^b
MRP-S10	P82664 (NP_060611)	AAF55148	T26634	S59279 (YDR041w)	?
MRP-S11	P82912 (NP_073750)	AAF55385	CAA99938	CAA54769 (YNL306w/MRP-S18)	P56802
MRP-S12	O15235	P10735	T24380	P53732 (YNR036C)	?
MRP-S14	O60783 (CAB16601)	CG112211	P49391	P10663 (MRP2/YPR166C)	P56804
MRP-S15	P82914	AAF46869	CAB97235	P21771 (YDR337W/MRPS28)	P56805
MRP-S16	Q9Y3D3 (AAD34127)	AAF58284	AAA81099	Q02608 (YPL013C)	P56806
MRP-S17	Q9Y2R5 (AAD27768)	AAF47177	AAB53829	Q03246 (YMR188C)	P16180
MRP-S18-(1)	Q9Y3D5 (AAD34129)	AAF57041	AAA91243	P40033 (YER050C)	P56807
MRP-S18-(2)	Q9Y676 (NP_054765)	AAF53877	CAA91421		
MRP-S18-(3)	Q9NVS2 (NP_060605)	AAF54251			
MRP-S21	P82921 (AF182417) ^c	AE003700 ^d	AAF99924	P38175 (YBL090W)	BAB01933
MRP-S22	P82650 (AAK01406)	AAF56757	CAB60995		
MRP-S23	XP_008155 (Q9Y3D9)		P34748	NP_012173 (YIL093C)	
MRP-S24	P82668	AAF56248			
MRP-S25	P82663 (BAB14968)	AAF48377	AAF60793	NP_012754 (YKL167C) ^e	
MRP-S26	CAC20860 (S78421) ^f	AAF49279			
MRP-S27	Q92552 (BAA13394)		CAB04602		
MRP-S28	P82673	AAF47688	CAB61063	NP_010460 (YDR175C)	
MRP-S29	P51398	AAF46846	CAB60994	Q01163 (YGL129C)	
MRP-S30 ^g	Q9NP92 (NP_057724)	AAF48515	T33116		
MRP-S31	Q92665 (NP_005821)	AAF49552			
MRP-S32 ^h	Q9Y6G3 (AAD44492)	AAF58852	T27551		
MRP-S33	Q9Y291 (AAD34134)	AAF55312	CAA91037		
MRP-S34	P82930	AAF49483	CAA84334		
MRP-S35	Q9Y2Q9 (NP_054737)	AAF57671	CAA21611		
MRP-S36	P82909 (AAG44788)		CAA21620	P19955 (YFR049W/YMR-31)	

^a EST number, full-length protein sequence cannot be found.

^b Possible chloroplast or mitochondrial location.

^c Twelve N-terminal residues are missing in the reported accession number.

^d *Drosophila* MRP-S21 homolog is encoded from two exons obtained from the complementary nucleotide sequences of this entry in between 9429 and 9110 bp.

^e Localized in the large subunit of yeast mitochondrial ribosomes (43).

^f Partial rat protein and bovine peptide fragment (6), respectively.

^g Found in both small and large subunits analysis. Subunit location of this protein is tentative (13).

^h Reported as a large subunit protein in Ref. 6.

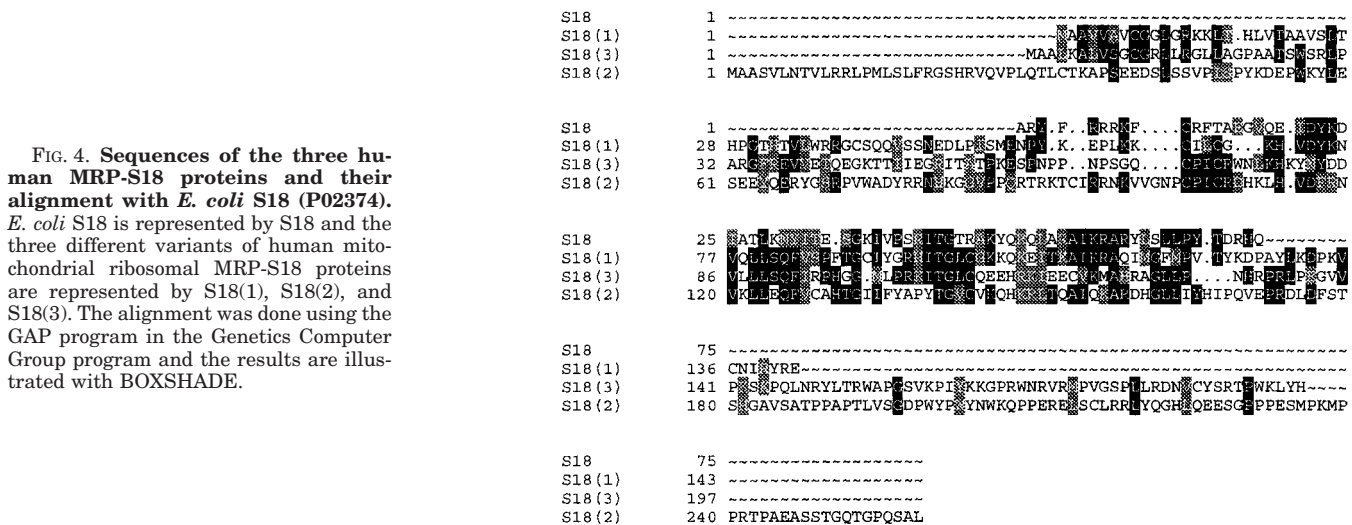


FIG. 4. Sequences of the three human MRP-S18 proteins and their alignment with *E. coli* S18 (P02374). *E. coli* S18 is represented by S18 and the three different variants of human mitochondrial ribosomal MRP-S18 proteins are represented by S18(1), S18(2), and S18(3). The alignment was done using the GAP program in the Genetics Computer Group program and the results are illustrated with BOXSHADE.

cially at the N-terminal end and in the central region (not shown). Human MRP-S6 is one of only two homologs that is shorter than its *E. coli* counterpart (Fig. 3).

MRP-S11—All the clones obtained from the virtual screening of the data bases by using any of the four peptides from MRP-S11 were described as “similar to 30 S ribosomal protein S11” (Table I). Human MRP-S11 is reasonably well conserved among the various mitochondrial sequences available (Table

III). The *S. cerevisiae* S11 homolog (YNL306w or MRP-S18) is 27% identical to *E. coli* S11. It has been defined as a mitochondrial ribosomal protein but not yet as an S11 homolog (27).

MRP-S15—Peptides derived from MRP-S15 were very abundant in the whole digests of 28 S subunit (Table I). Homologs of human MRP-S15 are readily detected in yeast, *D. melanogaster*, and *C. elegans* (Tables III and IV). The mitochondrial homologs of S15 are all considerably longer than bacterial S15

TABLE V
Percentage identity of human mitochondrial MRP-S18s to S18 families found in other species

S18	% Identity to														
	Human			<i>Drosophila</i>			<i>C. elegans</i>		Chloroplast Porpu*Arath ^a	<i>E. coli</i>	Strco		Myctu		
	1	2	3	1	2	3	1	2			1	2	1	2	
S18(1)		25.6	30.0	45.3	23.3	34.2	43.3	22.4	38.6	27.8	29.6	33.8	30.4	34.6	33.7
S18(2)	25.6		25.7	23.3	38.7	20	23.5	24.1	34.3	24.5	25.7	25.6	34.6	21.4	26.1
S18(3)	30.0	25.7		24.8	34.3	32.1	25	20.3	29.2	28.1	26	29.7	24.1	30.9	24.7

^a Chloroplast gene product.

The abbreviations used in this table are: Strco, *S. coelicolor*; Myctu, *M. tuberculosis*; Arath, *A. thaliana* (Mouse-ear cress); and Porpu, *P. purpurea* (red algae).

which is only about 88 residues in length (Fig. 3). Only a central region of MRP-S15 has homology to the bacterial proteins. The sequence of MRP-S15 is the least conserved of all the small subunit ribosomal proteins between human and mouse (Table III). Furthermore, less than 30% identity is observed between human MRP-S15 and the corresponding proteins from *D. melanogaster* and *C. elegans* (Table III).

MRP-S16—Two peptide sequences were sufficient to identify human MRP-S16 in the human ESTs (Table I). Human MRP-S16 is 40.2% identical to *E. coli* S16 with the sequences most highly conserved near the N terminus (Table III). Although MitoProt II predicts cleavage of a putative import signal at the residue 34 (Table II), the homology region of MRP-S16 with its bacterial homologs begins following residue 16 making it likely that the actual import signal is shorter than the predicted one. Homologs of human MRP-S16 are detectable in yeast, *D. melanogaster*, and *C. elegans* data bases (Table IV). MRP-S16 is one of the most highly conserved ribosomal proteins between mammalian and yeast mitochondria and the human MRP-S16 is about 40% identical to its bacterial homologs (Table III).

MRP-S17—Five peptides encoded by an unidentified mRNA (HSPC011) were identified. Subsequently, Swiss-Prot protein data bases searches using this unknown protein revealed that it is the mammalian mitochondrial ribosomal homolog of prokaryotic S17. Human MRP-S17 is moderately conserved among the mitochondrial and prokaryotic ribosomal proteins especially at the N-terminal and the central regions of the S17 family of proteins (Table III).

MRP-S18—In *E. coli* a single form of ribosomal protein S18 is observed. However, in other organisms such as *Streptomyces coelicolor* and *Mycobacterium tuberculosis*, two variants of S18 have been detected. Seven peptides derived from a mitochondrial S18 homolog were detected (Table I). These peptides hit both prokaryotic and chloroplast S18 ribosomal proteins. Somewhat surprisingly, the peptide sequences that were determined by mass spectrometry matched three different cDNA sequences encoding different proteins which are designated as MRP-S18(1), MRP-S18(2), and MRP-S18(3). The corresponding full-length human MRP-S18 proteins are deposited in GenBankTM. However, the functions of these proteins are listed as unknown.

Alignment of the three variants of MRP-S18 (Fig. 4) indicates the presence of conserved regions only in the central portion of the S18 proteins. The primary sequences of the three mitochondrial S18 variants are no more closely related to each other than they are to the prokaryotic S18s (Table V). Prokaryotic organisms such as *S. coelicolor* and *M. tuberculosis* also have more than one S18 homolog (Table III). Unlike the mitochondrial MRP-S18s, these prokaryotic homologs are greater than 50% identical to each other. Three MRP-S18 variants are present in mouse and *D. melanogaster* while two forms of this protein, corresponding to MRP-S18(1) and MRP-S18(2), are found in *C. elegans* (Table V). A single MRP-S18 appears to be present in yeast mitochondria. This protein, like the single S18 in *E. coli*, is more closely related to MRP-S18(1) than to the

other two forms (Table III). Human MRP-S18 proteins are more closely related to several chloroplast S18 proteins than to their prokaryotic S18 homologs (Table III). It is likely that each mitochondrial ribosome will have a single copy of MRP-S18. The presence of three variants of MRP-S18 suggests that there is a heterogeneous population of mitochondrial ribosomes.

MRP-S21—Searches performed with three peptides hit ESTs described as similar to 30 S ribosomal S21 protein and assembly of the cDNA sequences lead to the sequence of the full-length MRP-S21. Prokaryotic S21 proteins and the MRP-S21 homologs are well conserved in the central and the N-terminal regions. Yeast, *D. melanogaster*, and *C. elegans* homologs were found (Tables III and IV).

New Classes of Ribosomal Proteins in Mammalian Mitochondrial Ribosomes

MRP-S31—Six peptides were sequenced from the bovine mitochondrial ribosomes that correspond to a new class designated human MRP-S31 (Tables I and II). This protein was previously identified as "Imogen 38" (NP_065585) which is a 38-kDa mitochondrial autoantigen associated with type 1 diabetes (28, 29). Its relationship to the etiology of this disease remains to be clarified. The *D. melanogaster* homolog of this new class of mitochondrial ribosomal proteins is present. However, a *C. elegans* homolog could not be detected (Tables III and IV).

MRP-S32—A single peptide in the whole 28 S subunit digest lead to the identification of a new class of mitochondrial ribosomal protein designated MRP-S32. Homologs of MRP-S32 are found in a variety of other species although yeast does not appear to have a corresponding ribosomal protein. This observation is not surprising since several of the new classes of ribosomal proteins have not been observed in yeast (Tables III and IV).

MRP-S33—A single peptide (Table I) also allowed the identification of another new class of ribosomal proteins (MRP-S33). Again MRP-S33 has a high probability of being localized in mitochondria. MRP-S33 is one of the more highly conserved mitochondrial ribosomal proteins between mammals, flies, and worms (Table III). There is no detectable homolog to this protein in yeast mitochondrial ribosomes when searches are performed with mammalian, *Drosophila*, or *C. elegans* MRP-S33.

MRP-S36—Two peptides lead to the identification of the "new class" of ribosomal protein designated MRP-S36 (Table I). Like other new class mitochondrial ribosomal proteins, no homolog of this ribosomal protein can be detected in prokaryotes. However, MRP-S36 has a homolog in yeast (Tables III and IV) that has been identified as a mitochondrial ribosomal protein in previous studies (30). MRP-S36 is the fifth new class mitochondrial ribosomal protein that has a yeast homolog (Table III) (9, 12, 13). The *C. elegans* MRP-S36 homolog is detected in the *C. elegans* data bases (Table IV). No *Drosophila* homolog of MRP-S36 could be found probably due to high divergency of this ribosomal protein family in different species or due to a sequencing problem in the *Drosophila* data base.

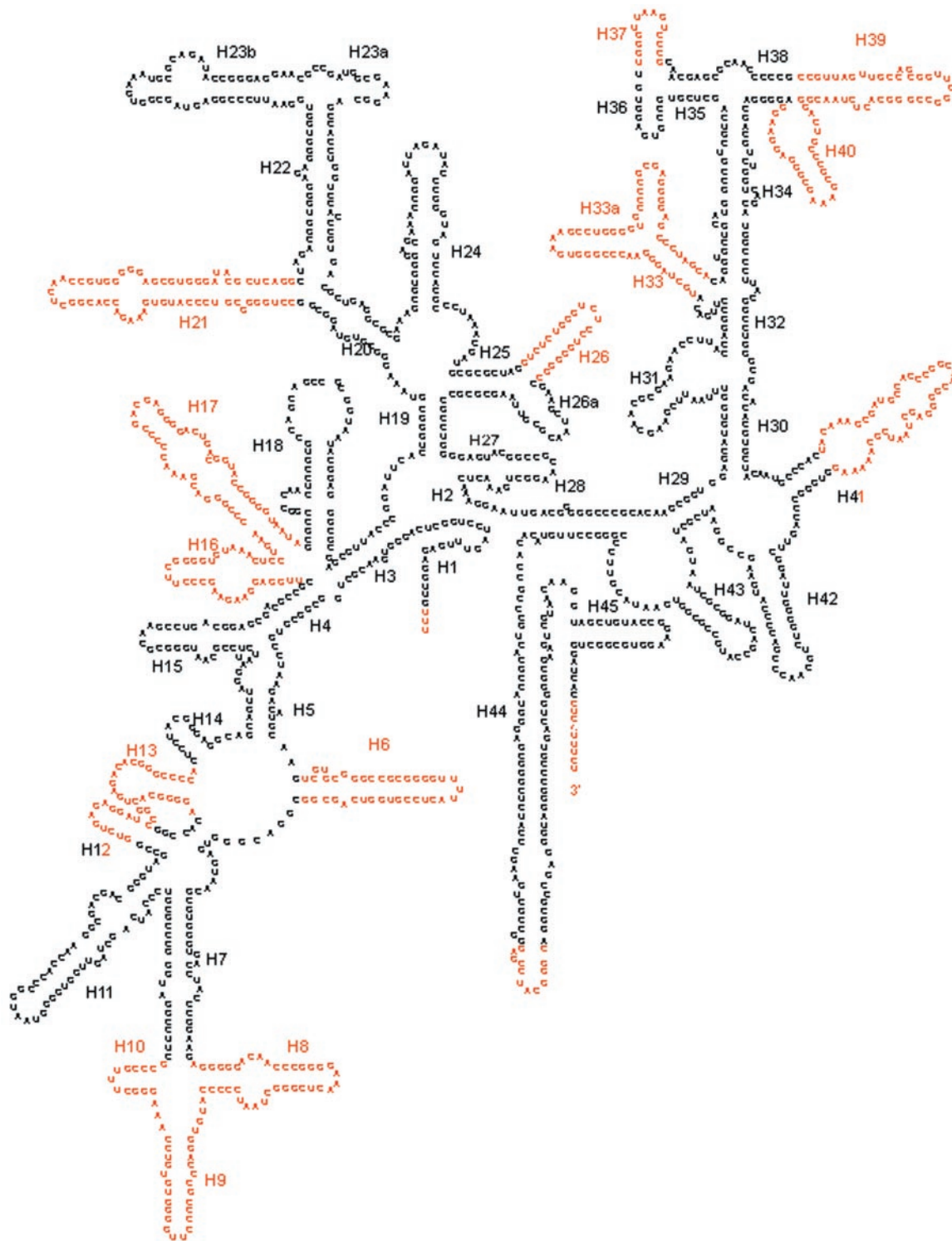


FIG. 5. Secondary structure comparison of ribosomal small subunit rRNAs of *T. thermophilus* 16 S rRNA and bovine mitochondrial 12 S rRNA. After superimposing the secondary structure of bovine mitochondrial 12 S rRNA on the *T. thermophilus* 16 S rRNA, the missing secondary structures in mitochondrial rRNA were colored in red (R. R. Gutell, S. Subashchandran, M. Schnare, Y. Du, N. Lin, L. Madabusi, K. Muller, N. Pande, N. Yu, Z. Shang, S. Date, D. Konings, V. Schweiker, B. Weiser, and J. J. Cannone, manuscript in preparation.) The remaining secondary structures are shown in black. Helix numbers are conserved in mitochondrial rRNA except that helix 22 (H22) does not form a perfect double helix in mitochondrial rRNA.

Other New Ribosomal Proteins

The current analysis of peptide digests of whole small subunits also lead to the confirmation of the presence of two small subunit ribosomal proteins reported previously (11). These ribosomal proteins were previously designated MRP-S12 and MRP-S28 (11). However, in the nomenclature we are proposing, MRP-S12 represents the mitochondrial homolog of pro-

karyotic S12. We, therefore, propose that this protein be designated as MRP-S34. The designation MRP-S28 was used previously to represent a different new class of mitochondrial protein and this sequence is designated as such in Swiss-Prot (12). Hence, we propose that this protein be identified as MRP-S35 (rather than MRP-S28). The peptides obtained from these two proteins are listed in Table I.

FIG. 6. The three-dimensional models of mitochondrial small subunit ribosomes based on the crystal structure of *T. thermophilus* 30 S subunit. The coordinates of the *T. thermophilus* 30 S subunit were obtained from the Protein Data Bank (accession number 1FJF) (32). In all the panels, the small subunit rRNA is represented by blue and red ribbons. Each model is shown in two different views (the front view representing the side of the small subunit that interacts with the large subunit and the back view). *A* and *B*, three-dimensional models of the *T. thermophilus* rRNA in the 30 S subunit showing the front view (*A*) and the back view (*B*) of the subunit, respectively. The blue regions are the conserved regions in both prokaryotic and mitochondrial rRNAs and the red regions are the portions missing in the mitochondrial small subunit rRNA. *C* and *D*, the prokaryotic ribosomal proteins that have homologs in mammalian mitochondrial ribosomes were located on the three-dimensional model of the 30 S subunit (green). Although mitochondrial ribosomes have an S21 homolog, this protein cannot be shown in this model due to the absence of S21 in *T. thermophilus*. The prokaryotic ribosomal proteins that do not have homologs in mammalian mitochondrial ribosomes are shown in yellow. Panel *C* is the front view (from the 50 S subunit side) while *D* is the back view of the small subunit. Again, regions of the 16 S rRNA present in the 12 S rRNA are shown in blue and regions missing are shown in red.

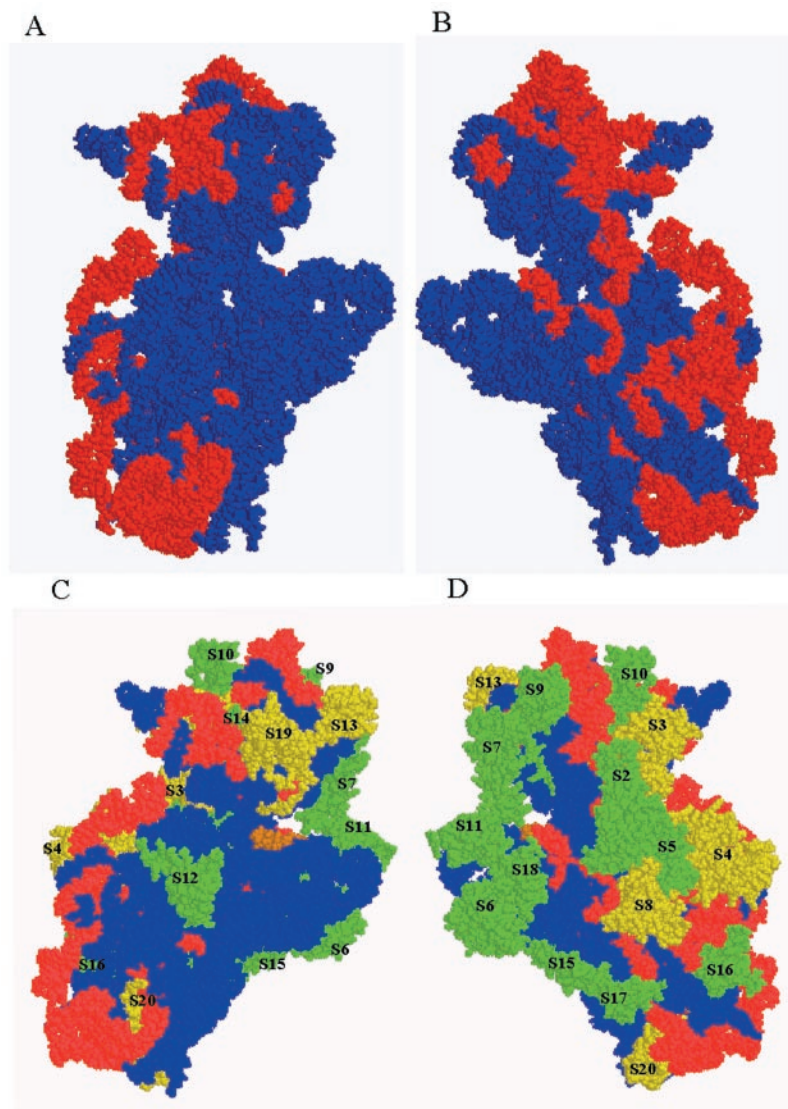


TABLE VI
Classification of mammalian mitochondrial ribosomal proteins according to their interaction with 12 S rRNA based on the 30 S structure (32)

Classification	Present	Absent
Primary	S7, S15, S17	S4, S8, S20
Secondary	S5, S6, S9, S12, S16, S18	S13, S19
Tertiary	S2, S10, S11, S14, S21	S3
Head (3' domain)	S2, S7, S9, S10, S14	S3, S13, S19
Platform (central domain)	S6, S11, S15, S18, S21	S8
Body (5' domain)	S5, S12, S16, S17	S4, S20

DISCUSSION

Eight ribosomal proteins described in this paper and 6 of the previously characterized mammalian mitochondrial ribosomal proteins show significant sequence similarities to bacterial ribosomal proteins. The remaining 15 proteins that have been identified in this and previous studies belong to new classes of ribosomal proteins (7–13). A large amount of new structural information on the ribosome allows us to begin to put these observations into a clearer structural context.

The mammalian mitochondrial 28 S subunit contains a 12 S rRNA which is 950 nucleotides in length compared with the 1542 residues in the *E. coli* 16 S rRNA. In general, the 12 S rRNA is not randomly shortened throughout its structure.

Rather, it shows striking deletions of a number of features of the secondary structure (Fig. 5) (31). The regions of 16 S rRNA present in the mitochondrial 12 S rRNA were examined using the three-dimensional model of the *Thermus thermophilus* 30 S subunit at 3-Å resolution to supply the coordinates (32). Front (large subunit interaction side) and back views are shown in Fig. 6, *A* and *B*, with the regions retained in the 12 S rRNA shown in blue and the regions missing shown in red. Most of the regions of the small subunit rRNA missing in the mammalian mitochondrial 12 S rRNA are located on the periphery of the subunit and on the back side away from the decoding region. RNA components creating the core structure of the platform, the front of the head, the neck, and part of the body have been retained in the 12 S rRNA. RNA in the central portion of the head, the spur, portions of the shoulder, and the edge of the body away from the platform are missing in the mitochondrial rRNA. The conservation of critical regions of the rRNA suggests that the basic functioning of the mitochondrial ribosome will be analogous to that of the bacterial ribosome.

Ribosomal proteins are classified in three categories depending on the order of their assembly into the subunits and the degree of their interaction with the rRNA. In the *E. coli* 30 S subunit, 6 proteins are classified as primary rRNA-binding proteins, 8 are classified as secondary rRNA-binding proteins while 6 are tertiary rRNA-binding proteins (Table VI). Classi-

fied in this way, mammalian mitochondrial ribosomes are missing 3 of the primary RNA-binding proteins, 2 of the secondary rRNA-binding proteins and only one of the tertiary RNA-binding proteins. S1 which is also missing in these ribosomes is not included in this tabulation.

The putative locations of the mitochondrial ribosomal proteins that have prokaryotic homologs have been examined using the model of the 30 S subunit (Fig. 6, C and D). This analysis indicates that truncation of the rRNA in the small subunit may account in part for the absence of certain ribosomal proteins but that a more complete understanding of structure/function relationships in this ribosome will be required before a clear interpretation of the data is possible. The body of the 30 S subunit contains the 5' domain and part of the 3' minor domain of the 16 S rRNA. The 5' domain of the rRNA interacts primarily with 6 proteins (Table VI). Homologs of 4 of these proteins are present in mammalian mitochondrial ribosomes. These are clustered primarily near the junction of the body with the head and platform of the subunit (Fig. 6). Two of the primary RNA-binding proteins missing in the 28 S subunit (S4 and S20) would have been localized in the body of the subunit (yellow in Fig. 6).

The lack of S4 in mammalian mitochondrial ribosomes is rather surprising. S4 is important for the accuracy of translation and mutations in S4 can cause an increase in misreading (33). S4 binds to a five-way junction between H3, H4, H16, H17, and H18 in the 5' domain of the 16 S rRNA (32). It is also in contact with H21. The 12 S rRNA in mammalian mitochondria lacks H16 and H17 suggesting that this region of the small subunit may have a structure somewhat different from that observed in bacterial ribosomes. S4 normally makes strong contacts with S5 in the body of the subunit as part of a three-way interaction S4-S5-S8. Of these three, only S5 has been retained in the 28 S subunit. It is possible that the large size of MRP-S5 compared with prokaryotic S5 (Fig. 3) may arise from the loss of S4 and S8.

A homolog of S20 found in the body of the small subunit is also missing in the human mitochondrial ribosome (Fig. 6). In prokaryotic ribosomes, S20 which is a primary RNA-binding protein is located near the bottom of the body. Two of the major helices in contact with S20 (H6 and H8) are missing in the 12 S rRNA perhaps accounting in part for the lack of S20.

The central domain of the 16 S rRNA forms the platform of the 30 S subunit which is involved in forming the P-site. Five of the 6 proteins located in this region of the 30 S subunit are present in the mammalian mitochondrial ribosome (Table VI and Fig. 6). Thus, the core ribonucleoprotein structure of the platform has been well conserved in the mitochondrial ribosome. Three variants of S18 located in this region of the small subunit have been observed in our studies. In bacterial ribosomes, S18 undergoes a conformational change upon the binding of mRNA to the small subunit (34). The observation that three variants of S18 have been located in human mitochondrial ribosomes raises the possibility that they may confer different mRNA binding properties on subpopulations of small subunits.

Only one protein located primarily on the platform of the small subunit, the primary rRNA-binding protein S8, is missing in the mitochondrial ribosome (Fig. 6, Table VI). S8 interacts with H21 which is missing in mitochondrial 12 S rRNA (Fig. 5). S8 is not required for assembly of any other ribosomal proteins on the 16 S rRNA (35, 36) although it does form strong electrostatic contacts with S5.

The head and neck regions of the small subunit are formed by the 3' domain of the 16 S rRNA (32, 37). This region contains 8 proteins of which 5 have been preserved in the mammalian

mitochondrial ribosome (Table VI). The only primary RNA-binding protein in this region (MRP-S7) has been conserved. S7 has been implicated as forming part of the E-site. S7 potentiates the binding of S9, S10, and S14 near the top of the head all of which have been retained in the 28 S subunit.

The missing secondary and tertiary rRNA-binding proteins in the head region are the homologs to S13, S19, and S3 (Table VI and Fig. 6). S13 and S19 are located close to each other in the head of the 30 S subunit (32). S13 and S19 are able to cross-link to tRNA at the A and P sites (38). Moreover, S19 and S13 are the only protein components that are located in the front of the head of the 30 S subunit where it interacts with the central protuberance of the 50 S subunit. Apparently, the functions of these proteins have been replaced by a new class ribosomal proteins in mammalian mitochondria. The absence of S3 is somewhat surprising since most of the regions of the small subunit rRNA that it interacts with (except H16) have been preserved in the 12 S rRNA. Furthermore, S3 contacts S10 and S14 in the head forming a tight cluster held by hydrophobic interactions. Both S10 and S14 are present in the small subunit of the mammalian mitochondrial ribosome. MRP-S10 is quite a bit larger than its bacterial counterpart and a portion of the role of S3 may have been assumed by the additional sequences present in MRP-S10. In prokaryotes, S3 has been implicated in the assembly of the 30 S subunit but may not be essential once assembly is completed (39).

Half of the proteins identified in mammalian mitochondrial ribosomes do not have prokaryotic homologs. Some of these may have replaced specific prokaryotic ribosomal proteins during evolution serving related functions. Some of these new ribosomal proteins also appear to have evolved additional roles for the cell. For example, MRP-S29 also known as the death-associated protein 3 is involved in apoptosis (40, 41). MRP-S31 (Imogen 38, described in this report) has been found to be associated with type 1 diabetes (29). These observations suggest that components of the mitochondrial protein biosynthetic system may play a pivotal role in apoptosis and mitochondrial diseases. They may also play a role in coordinating mitochondrial gene expression with the metabolic needs of the cell. The roles and locations of all these new class ribosomal proteins remain to be determined.

Acknowledgment—We thank Mary Moyer for excellent technical assistance with the protein sequence analysis.

REFERENCES

- Pel, H., and Grivell, L. (1994) *Mol. Biol. Rep.* **19**, 183–194
- De Vries, H., and van der Koogh-Schuurin, R. (1973) *Biochem. Biophys. Res. Commun.* **54**, 308–314
- O'Brien, T. W., Mathews, D. E., and Denslow, N. D. (1976) in *Genetics and Biogenesis of Chloroplasts and Mitochondria* (Bucher, T. L., Neupert, W., Sebald, W. S., and Werner, S., eds) pp. 741–748, Elsevier, Amsterdam
- Matthews, D. E., Hessler, R. A., Denslow, N. D., Edwards, J. S., and O'Brien, T. W. (1982) *J. Biol. Chem.* **257**, 8788–8794
- Cahill, A., Baio, D., and Cunningham, C. (1995) *Anal. Biochem.* **232**, 47–55
- Goldschmidt-Reisin, S., Kitakawa, M., Herfurth, E., Wittmann-Liebold, B., Grohmann, L., and Graack, H.-R. (1998) *J. Biol. Chem.* **273**, 34828–34836
- Graack, H.-R., Bryant, M., and O'Brien, T. W. (1999) *Biochem.* **38**, 16569–16577
- Koc, E. C., Blackburn, K., Burkhart, W., and Spremulli, L. L. (1999) *Biochem. Biophys. Res. Commun.* **266**, 141–146
- Koc, E. C., Burkhart, W., Blackburn, K., Moseley, A., Koc, H., and Spremulli, L. L. (2000) *J. Biol. Chem.* **275**, 32585–32591
- Mariottini, P., Shah, Z. H., Toivonen, J., Bagni, C., Spelbrink, J., Amaldi, F., and Jacobs, H. (1999) *J. Biol. Chem.* **274**, 31853–31862
- O'Brien, T. W., Liu, J., Sylvester, J., Mourgey, E. B., Fischel-Ghodsian, N., Thiede, B., Wittmann-Liebold, B., and Graack, H.-R. (2000) *J. Biol. Chem.* **275**, 18153–18159
- Koc, E. C., Burkhart, W., Blackburn, K., Koc, H., Moseley, A., and Spremulli, L. L. (2001) *Prot. Sci.* **10**, 471–481
- Koc, E. C., Ranasinghe, A., Burkhart, W., Blackburn, K., Koc, H., Moseley, A., and Spremulli, L. L. (2001) *FEBS Lett.* **492**, 166–170
- Tong, W., Link, A., Eng, J. K., and Yates, J. R. (1999) *Anal. Chem.* **71**, 2270–2278
- Shevchenko, A., Wilm, M., Vorm, O., and Mann, M. (1996) *Anal. Chem.* **68**, 850–858

16. Burkhart, W. (1992) in *Techniques in Protein Chemistry IV* (Angeletti, R., ed) pp. 399–406, Academic Press, New York
17. Perkins, D. N., Pappin, D. J., Creasy, D. M., and Cotrell, J. S. (1999) *Electrophoresis* **20**, 3551–3567
18. Pearson, W. R., and Lipman, D. J. (1988) *Proc. Natl. Acad. Sci. U. S. A.* **85**, 2444–2448
19. Jiang, X., Smith, J. B., and Abraham, E. C. (1996) *J. Mass Spec.* **31**, 1309–1310
20. Altschul, S. F., Madden, T. L., Schaffer, A. A., Zhang, J., Zhang, Z., Miller, W., and Lipman, D. J. (1997) *Nucleic Acids Res.* **25**, 3389–3402
21. Nakai, K., and Kanehisa, M. (1992) *Genomics* **14**, 897–911
22. Claros, M. G., and Vincens, P. (1996) *Eur. J. Biochem.* **241**, 770–786
23. Yamaguchi, K., von Knoblauch, K., and Subramanian, A. R. (2000) *J. Biol. Chem.* **275**, 28455–28465
24. Yamaguchi, K., and Subramanian, A. R. (2000) *J. Biol. Chem.* **275**, 28466–28482
25. Pietromonaco, S., Denslow, N., and O'Brien, T. W. (1991) *Biochimie (Paris)* **73**, 827–836
26. Behal, R. H., DeBuysere, M. S., Demeler, B., Hansen, J. C., and Olson, M. S. (1994) *J. Biol. Chem.* **269**, 31372–31377
27. Graack, H.-R., and Wittmann-Liebold, B. (1998) *Biochem. J.* **329**, 433–448
28. Lithgow, T. (2000) *FEBS Lett.* **476**, 22–26
29. Arden, S. D., Roep, B. O., Neophytou, P. I., Usac, E. F., Duinkerken, G., de Vries, R. R., and Hutton, J. C. (1996) *J. Clin. Invest.* **97**, 551–561
30. Matsushita, Y., Kitakawa, M., and Isono, K. (1989) *Mol. Gen. Genet.* **219**, 119–124
31. Zweib, C., Glotz, C., and Brimacombe, R. (1981) *Nucleic Acids Res.* **9**, 3621–3640
32. Wimberly, B. T., Brodersen, D. E., Clemons, W. M. J., Morgan-Warren, R. J., Carter, A. P., Vornrhein, C., Hartsch, T., and Ramakrishnan, V. (2000) *Nature* **407**, 327–339
33. van Acken, U. (1975) *Mol. Gen. Genet.* **140**, 61–68
34. Kang, C., Wells, B., and Cantor, C. R. (1979) *J. Biol. Chem.* **254**, 6667–6672
35. Koehler, C. M. (2000) *FEBS Lett.* **476**, 27–31
36. Allard, P., Rak, A. V., Wimberly, B. T., Clemons, W. M. J., Kalinin, A., Helgstrand, M., Garber, M. B., Ramakrishnan, V., and Hard, T. (2000) *Struct. Fold. Des.* **8**, 875–882
37. Schluenzen, F., Tocilj, A., Zarivach, R., Harms, J., Gluehmann, M., Janell, D., Bashan, A., Bartels, H., Agmon, I., Franceschi, F., and Yonath, A. (2000) *Cell* **102**, 615–623
38. Osswald, M., Doring, T., and Brimacombe, R. (1995) *Nucleic Acids Res.* **23**, 4635–4641
39. Ramakrishnan, V., Graziano, V., and Capel, M. S. (1986) *J. Biol. Chem.* **261**, 15049–15052
40. Kissil, J. L., Deiss, L. P., Bayewitch, M., Raveh, T., Khaspekov, G., and Kimchi, A. (1995) *J. Biol. Chem.* **270**, 27932–27936
41. Kissil, J. L., Cohen, O., Raveh, T., and Kimchi, A. (1999) *EMBO J.* **18**, 353–362
42. Shah, Z. H., O'Dell, K. M. C., Miller, S., An, X., and Jacobs, H. T. (1997) *Gene (Amst.)* **204**, 55–62
43. Fearon, K., and Mason, T. L. (1992) *J. Biol. Chem.* **267**, 5162–5170
44. Genetics Computer Group (1999) *Wisconsin Package version 10*, Genetics Computer Group, Madison WI